Biosensors and Bioelectronics 126 (2019) 535–542

Contents lists available at ScienceDirect

Biosensors and Bioelectronics

journal homepage: www.elsevier.com/locate/bios

Silver coordination complex amplified electrochemiluminescence sensor for sensitive detection of coenzyme A and histone acetyltransferase activity

Hongjun Chen[a,b], Xiu Liu[c], Wang Li[b,d,*], Yan Peng[e], Zhou Nie[b]

[a] Hunan Provincial Key Laboratory of Fine Ceramics and Powder Materials, School of Materials and Environmental Engineering, Hunan University of Humanities, Science and Technology, Loudi 417000, PR China
[b] State Key Laboratory of Chemo/Biosensing and Chemometrics, College of Chemistry and Chemical Engineering, Hunan University, Changsha 410082, PR China
[c] Key Laboratory of Pesticide Harmless Application, Collaborative Innovation Center for Field Weeds Control (CICFWC) of Hunan Province, Hunan University of Humanities, Science and Technology, Loudi 417000, PR China
[d] National Engineering Laboratory for Deep Process of Rice and Byproducts, Central South University of Forestry and Technology, Changsha 410004, PR China
[e] College of Economics and Management, Hengyang Normal University, Hengyang 421008, PR China

ARTICLE INFO

Keywords:
Silver coordination complex
ECL amplification
Signal-on
Histone acetyltransferase

ABSTRACT

A kind of coenzyme A (CoA)-silver coordination complex (CoA-Ag) was in-situ developed and verified to accelerate the electron transferring and electrochemical catalysis of H_2O_2 decomposition to enhance the cathode ECL intensity of CdTe@CdS QDs. Afterward, a convenient label-free signal-on ECL approach was constructed for CoA detection with excellent specificity. In addition, the unique ECL enhancing phenomenon was also proposed to assay the enzymatic activity of histone acetyltransferases (HAT) and screen relevant inhibitors, exhibiting a promising potential in the practical application of biochemical research, disease diagnosis and drug discovery.

1. Introduction

Reversible protein acetylation on lysine residues that regulated by the antagonistic catalytic activity of histone acetyltransferases (HATs) and histone deacetylases (HDACs) is an essential post-translational modification (Li et al., 2016). Aberrant expression and dysregulation of HATs/HDACs are associated with a range of diseases, such as neurological disorders, metabolic syndrome cancer and chronic inflammation (Biel et al., 2005). Inspired by the great significance of HATs/HDACs, plenty of assay technologies have been developed to evaluate the enzyme activity. Traditional radiometric assays were proposed with intrinsic hazards of radioactive materials application and multistep laborious procedures (Li et al., 2016). Other innovative nonisotopic methods including ELISA, fluorescence, colorimetry and electrochemical method usually dependent on the specific biorecognition proteins including acetylation-specific antibodies or protein domains (Ghadiali et al., 2011; Kuninger et al., 2007; Trievel et al., 2000; Wang et al., 2015; Wu et al., 2012; Wu and Zheng, 2008; Zhen et al., 2012). Alternative fluorescence methods based on the indirect quantization of by-products such as coenzyme A (CoA) usually require fluorescent labeling and be susceptible to other sulfhydryl interferences (Gao et al., 2013).

Electrochemical techniques have attracted broad attention for their outstanding advantages, such as satisfactory sensitivity and convenient operation. Nowadays, nucleic acid nanostructures such as DNA tetrahedron structure, nucleic acid-mimicking structure, exhibit noticeable application in the field of post-translational modification electrochemical sensing (Chen et al., 2017a, 2017b; Hu et al., 2015; Pei et al., 2010, 2011; Wang et al., 2016, 2017). In particular, RNA-mimicking coordination nanostructure is reported for enzymatic activity (HAT and citrate synthase) electrochemical label-free biosensing (Hu et al., 2015; Wang et al., 2017). Electrochemiluminescence (ECL) combining electrochemical and optical techniques possessing advantages in simple operation, fast response, low background, high sensitivity and low instrument requirements, is currently a promising technique for biosensing (Benoit and Choi, 2017; Liu et al., 2015). While, limited investigations are reported on HAT activity detection employing ECL strategy. Inspired by the consideration, construction an ECL biosensor for HAT activity detection and related inhibitors assessment is of great importance.

With respect to ECL sensing, considerable parts of them are turn-off with the signal quenching systems, and commonly lack of efficient signal-to-noise ratio (Zheng et al., 2016). While, signal-on sensing possesses advantages in improved target recognition and sensitivity,

* Corresponding author at: National Engineering Laboratory for Deep Process of Rice and Byproducts, Central South University of Forestry and Technology, Changsha 410004, PR China.
E-mail address: wli@hnu.edu.cn (W. Li).

https://doi.org/10.1016/j.bios.2018.11.003
Received 3 September 2018; Received in revised form 25 October 2018; Accepted 2 November 2018
Available online 09 November 2018
0956-5663/

and becomes trend in ECL sensor construction. Apparently, ECL signal amplification designation is essential for sensor fabrication. Nano-materials hold the essential catalysis due to their large specific surface area and high surface energy, exhibiting a prominent application for ECL signal amplification (Benoit and Choi, 2017; Ding et al., 2015; Jie et al., 2017; Xu et al., 2018). Recently, a kind of CoA-Ag complex synthesized by thiol-Ag interaction was used for optical and electrochemical biosensors construction (Hu et al., 2015, 2017a, 2017b; Wang et al., 2016). However, application of CoA-Ag complex in ECL for HAT enzymatic activity biosensing is missed.

Herein, we synthesize CoA-Ag complex to study the magnifying capability on the cathodic ECL signals of CdTe@CdS quantum dots (CdTe@CdS QDs). Furtherly, the ECL enhancing mechanism was further investigated in-depth. Related findings enable us to further develop the label-free signal-on ECL approaches for histone acetyltransferase detection and its inhibitors assessment.

2. Materials and methods

2.1. Chemicals and apparatus

Graphite powder (99.99%, 325 meshes) was available from Alfa Aesar. The graphene oxide (GO) used in this work was prepared following Hummer's method (Hummers and Offeman, 1958). Histone acetyltransferase p300 (HAT), CoA, CoA assay kit and acetyl-CoA were purchased from Sigma-Aldrich. The ECL data were recorded at room temperature through MPI-A Multifunctional Electrochemical and Chemiluminescence Analysis System (Remex Corporation, Xi'an, China), and its emission window is −800 V. CHI660A electrochemical workstation (Shanghai, China) was used for each electrode modification. A conventional three-electrode system, glassy carbon electrode (GE) was invoked as the working electrode, the platinum wire electrode was the auxiliary electrode and Ag/AgCl (saturated KCl solution) was the reference electrode. Core-like CdTe@CdS QDs was one-pot prepared in aqueous (Chen et al., 2012) and characterized in supplementing information (Fig. S1). All solutions were prepared with ultrapure water (18.25 MΩ cm), which was obtained from a Millipore Milli-Q system.

2.2. Synthesis and characterization of CoA-Ag complex

The CoA-Ag complex was synthesized according to the following procedures: $AgNO_3$ (1 mM, 10 μL) and CoA (1 mM, 10 μL) was added to phosphate buffer (10 mM, pH 7.0) with a total reaction volume of 100 μL. And then shaken for 8 min (500 rpm) on a 30 °C constant temperature magnetic stirrer. After the reaction, the CoA-Ag complex was obtained and stored at 4 °C.

The complex was characterized by fluorescence, hydrated particle size and atomic force microscopy. In the fluorescence experiment, 2 μL SGII (1:100) was added to 98 μL of synthesized CoA-Ag complex. After mixing and incubation for 20 min, the fluorescence spectra were measured at 494 nm excitation wavelengths. Atomic force microscopy (AFM) was carried out by mixing GO suspension (0.5 mg/mL) with a certain amount of CoA-Ag complex solution, centrifuging for 10 min (10,000 r/min) to disperse the precipitate again in water, taking 10 μL drops on the mica sheet at 37 °C constant temperature drying.

2.3. Preparation of CdTe@CdS/CoA-Ag/GO modified electrode

The glassy carbon electrode (GE) was firstly polished with a polystyrene polished cloth of 1.0, 0.3 and 0.05 μm respectively, and then cleaned twice in ethanol and water for 5 min each time. After that, placing clean GE in GO solution (1.0 mg/mL) and electrodeposited for 800 s at −1.3 V with a potentiostatic method to electrodeposite GO onto GE surface (GO/GE). The physically adsorbed GO was removed with ultrapure water rinsing. Then, 2 μL of the prepared CoA-Ag complex was dropped onto GO/GE electrode surface, incubated 30 min at room temperature and rinsed with ultrapure water (CoA-Ag/GO/GE). Finally, 2 μL of CdTe@CdS QDs containing 0.5% chitosan was added to CoA-Ag/GO/GE surface and dried (CdTe@CdS/CoA-Ag/GO/GE). The aforementioned electrodes were used for the subsequent electrochemical and ECL experiments.

2.4. Quantitative detection of CoA

A series different concentration of CoA was mixed with $AgNO_3$ (100 μM) and reacted for 8 min under shocking in accordance with the above preparation of CoA-Ag complex method. Then, 2 μL of CoA-Ag reaction solution above was dropped to the GO/GE electrode surface, incubated at room temperature for 30 min and rinsed with water forming a series different CoA-Ag complex modified electrode (CoA-Ag/GO/GE). After that, 2 μL of CdTe@CdS QDs prepared in 0.5% chitosan was added to the above CoA-Ag/GO/GE and dried for the final ECL detection. Briefly, the electrodes were placed in PBS (pH 8.0, 200 mM) containing 5 mM H_2O_2 and subjected to cyclic voltammetry with scanning between −0.5 V and −1.4 V potential at a sweep speed of 50 mV s^{-1}.

2.5. Acetyltransferase p300 activity detection and its inhibitors assessment

Activity of acetyltransferase p300 was performed as follows. First, different concentrations of p300 (0.1, 0.5, 1.0, 5.0, 10, 20, 50, 100 and 150 nM) were incubated with 200 μM substrate peptides H4 and 500 μM acetyl coenzyme A in phosphate buffer solution (10 mM, pH 7.0) (total volume 100 μL). The mixture was then incubated in 30 °C water baths for 80 min to complete enzymatic reaction. Afterward, 1 μL silver nitrate (50 mM) was rapidly injected into the above solution under shocking and reacted for 8 min to prepare CoA-Ag complex. Subsequently, 2 μL of the above reaction solution containing CoA-Ag product was dropped on the GO/GE electrode incubating for 30 min and rinsed with water. The following procedures were the same as previously mentioned.

For the inhibitor assessment, HAT p300 (100 nM), substrate peptides H4 (200 μM), and anacradic acid at different final concentrations (1.0, 5.0, 10, 25, 50, 75, 100, 150 and 200 μM) were pre-incubated for 10 min at room temperature, and then the reaction was initiated by the addition of Ac-CoA (500 μM) and $AgNO_3$ (500 μM) in PBS buffer (10 mM, pH 7.0) with a total volume of 100 μL at 30 °C for 80 min. The following procedures were the same as previously mentioned.

3. Results and discussion

3.1. Synthesis and verification of CoA-Ag complexes

A series of mercapto-metal complexes are synthesized resorting mercapto functional group ligation with metal because of the reactive ability of mercapto substance with noble metal (such as silver, gold, copper) ions (Ma et al., 2018; MacDonald et al., 2011; Mishra and Drueckhammer, 2000; Yuan et al., 2013). Coenzyme A is an essential coenzyme in the metabolism, which is consisting of adenosine 3′-phosphate and a mercapto group in its section. Consequently, CoA can be considered as a kind of mercapto group functional compounds possessing the ability to synthesis of mercapto-Ag complex (Hu et al., 2015). In view of the aforementioned principle, two functional groups mercapto and adenine groups are connected at the end of CoA molecule, it is reasonable to supposed that the resultant CoA-Ag complex has some special properties of being composed of a large number of mercapto-Ag repeating units and resembling to the analogous poly-A RNA strand.

In order to verify the RNA-like structure of CoA-Ag complex, we firstly investigated whether the synthesized CoA-Ag complex can be bound to SGII with fluorescent method because SGII fluorescent dyes can specifically stains single-stranded nucleic acids (Chen et al.,

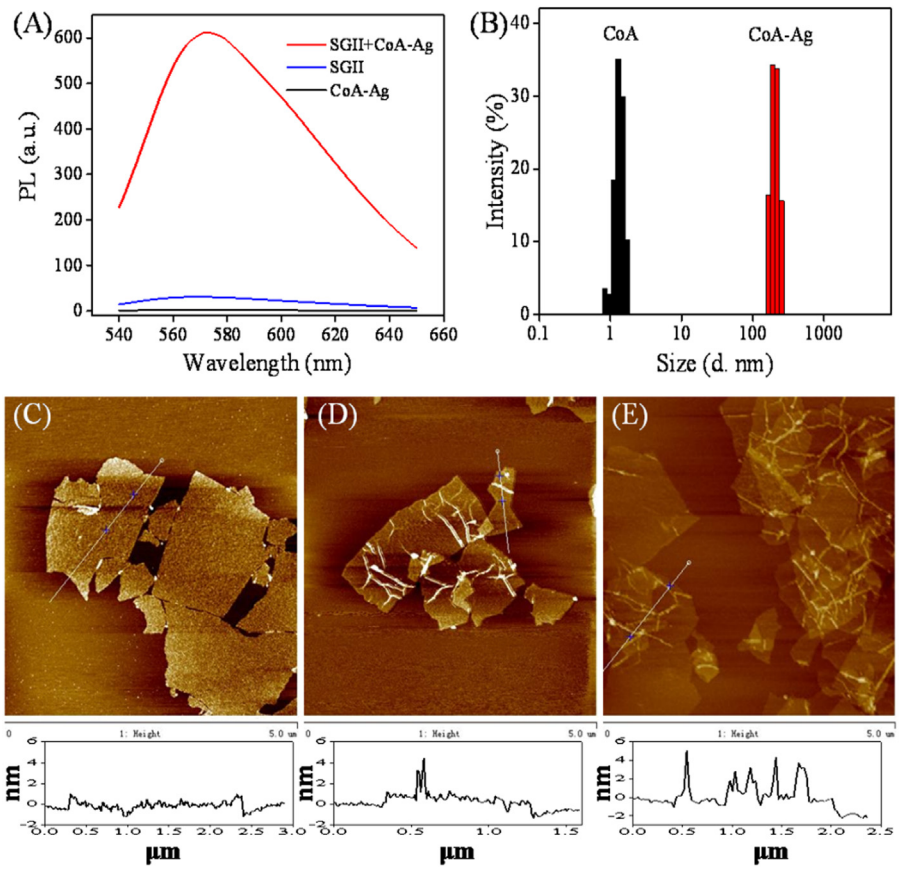

Fig. 1. (A) Fluorescence spectra of sole SGII solution (blue curve), and the as-prepared CoA-Ag complex (CoA-Ag, 100 μM) (λex = 494 nm) in the presence (red curve) and absence (black curve) of SGII (1:100). (B) Size distribution of CoA-Ag determined by dynamic light scattering (DLS). AFM images of GO (C), and GO with 5 mM (D) and 10 mM (E) concentration of CoA-Ag complex. Line charts in the bottom of these AFM images are associated height profiles (For interpretation of the references to color in this figure legend, the reader is referred to the web version of this article).

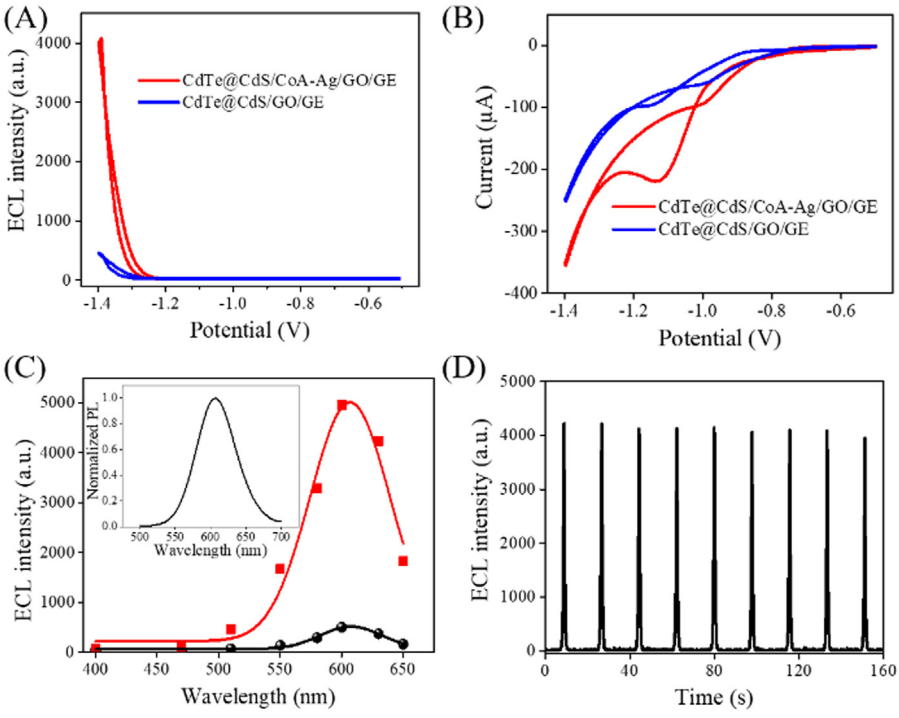

Fig. 2. (A) ECL-potential curves and (B) cyclic votammertry curves of CdTe@CdS QDs modified GO/GE with (red line) and without (blue line) CoA-Ag complex modification. (C) ECL peak spectra of cathodic responses collected on CdTe@CdS QDs modified GO/GE with (red line) and without (black line) CoA-Ag complex modification, which obtained by the optical filter (inset shows the normalized fluorescent spectrum of CdTe@CdS QDs). (D) ECL-time curve of the CdTe@CdS/CoA-Ag/GO/GE continuously scans for 9 cycles (For interpretation of the references to color in this figure legend, the reader is referred to the web version of this article).

2015b). As shown in Fig. 1A, a remarkably amplified signal emission was obtained for CoA-Ag complex with SGII, while single CoA-Ag complex or SGII possesses inapparent fluorescence. The results verify that the synthesized CoA-Ag complex has a structure of RNA. Afterward, different batches of the synthesized CoA-Ag complex exhibit little differences in PL intensity (Fig. S2), indicating a proper preparing producibility. In addition, as shown in Fig. 1B, a clear increase in hydrated particle size obtains in comparison to the individual coenzyme A, further confirming the synthesis of the CoA-Ag complex. Moreover, a large number of curled nanowires with linear crystal structure are presented (Fig. S3), which intuitively confirm the nanowire like structure of CoA-Ag complex. Consequently, it can be concluded that CoA-Ag

complex is synthesized with an RNA structural similarity (Hu et al., 2015; Wang et al., 2016).

It is reported that single-stranded nucleic acid is easily adsorbed on graphene or graphene oxide (GO) surface by means of π-π stack and intermolecular force (Han et al., 2015; Hu et al., 2015). As CoA-Ag complex is analogous to RNA, it is reasonable to speculation on the highly adsorption ability onto the GO surface. As shown in Figs. 1D and 1E, a number of linear nanowires with 2 ~ 4 nm in height are randomly loaded on GO surface, intuitively demonstrating that CoA-Ag complex is a chain structure analogous to nucleic acid strand. In particular, nearly all nanowires are uploaded onto the GO sheet surface while little on the substrate may be due to powerful π-π interactions between stacked adenine and GO framework. Moreover, as shown in Fig. 1E, the amounts of CoA-Ag complex loaded on GO increase with the increment of CoA-Ag complex, suggesting a promising sensing application.

3.2. CoA-Ag complex enhanced electrochemiluminescence of CdTe@CdS QDs

CdTe@CdS QDs is a type of cathodic ECL emissive nanomaterial (Chen et al., 2015a). Investigations on the ECL signal amplification behavior of CdTe@CdS QDs towards CoA-Ag complex is insufficient. Therefore, CoA-Ag complex was introduced into CdTe@CdS QDs-ECL system to investigate the electrochemical and ECL behaviors. As shown in Fig. 2A, CdTe@CdS QDs shows an initial emission potential at −1.3 V and reaching to the highest ECL emission at −1.4 V. Once CoA-Ag complex was modified, a 9-time remarkably enhanced ECL signal was obtained, indicating the promising application potential for turn-on ECL sensing construction. In addition, the relative electrochemical behaviors essential to ECL emissive mechanism were further investigated (Fig. 2B). CdTe@CdS QDs alone exhibits an obvious reduction current peak at −1.1 V (blue line) belonging to the reduction of peroxide hydrogen (He et al., 2013), and generates a shape reduction current after −1.3 V which is in consistence with its initial ECL potential. Surprisingly, a significant CV current increase arises in the presence of CoA-Ag complex (red line), indicating faster electron transfer rate is arisen from CoA-Ag complex.

CdTe@CdS QDs exhibits an ECL maximum wavelength at 607 nm (black line, Fig. 2C), which is comparable to the fluorescent emissive spectrum (Fig. 2C inset) indicating the cathodic ECL signal originates from CdTe@CdS QDs excited state (CdTe@CdS*). In the presence of CoA-Ag complex, CdTe@CdS QDs exhibits a same maximum wavelength at 607 nm. Therefore, the CoA-Ag complex just amplify the amount of CdTe@CdS*, but never change other attributes of CdTe@CdS QDs. After all, it is speculated that the CoA-Ag complex accelerates the electron transfer on the electrode surface to raise the number of CdTe@CdS*, and finally enhances the ECL signal. The ECL signal stability was studied to verify the application potentiality for the proposed CoA-Ag complex enhanced system. The enhancing system displays stable ECL signal (Fig. 2D) with a relative standard deviation of 2% at cathodic potential during 9 cycles of sequential voltage scans, demonstrating good stability and reliability for ECL reactions and solid foundation for sensor construction.

3.3. CoA-Ag complex amplified ECL mechanism of CdTe@CdS QDs

As depicted earlier, CoA-Ag complex is speculated to accelerate the electron transfer on the electrode surface increasing the number of CdTe@CdS*, and finally enhance the ECL signal of CdTe@CdS QDs. The ECL emission mechanism of CdTe@CdS QDs employing H_2O_2 as the coreactant has been wildly reported and detailedly illustrated as follows (Eqs. (1)–(5)) (Bae et al., 2004; Jie et al., 2007). Briefly, the coreactant H_2O_2 was reduced to the hydroxyl radicals (•OH) (Eq. (1)) and the CdTe@CdS QDs were reduced to nanocrystal species (CdTe@CdS(e^-)) by charge injection (Eq. (2)) during negative potential direction scanning. Subsequently, excited state CdTe@CdS* was generated due to •OH reacts with the negatively charged CdTe@CdS(e^-) (Eq. (3)) or H_2O_2 directly oxidizes CdTe@CdS QDs (Eq. (4)), and synchronously emitted light (Eq. (5)).

ECL emission processes

$$H_2O_2 + e^- \rightarrow \cdot OH + OH^- \quad (1)$$

$$CdTe@CdS + e^- \rightarrow CdTe@CdS(e^-) \quad (2)$$

$$CdTe@CdS(e^-) + \cdot OH \rightarrow CdTe@CdS^* + OH^- \quad (3)$$

or

$$2CdTe@CdS(e^-) + H_2O_2 \rightarrow 2CdTe@CdS^* + 2OH^- \quad (4)$$

$$CdTe@CdS^* \rightarrow CdTe@CdS + hv \quad (5)$$

Hydrogen peroxide electrochemical reduction

$$H_2O_2 + e^- \rightarrow \cdot OH + OH^- \quad (6)$$

$$\cdot OH + e^- \rightarrow OH^- \quad (7)$$

According to the above mechanism, H_2O_2 and •OH is critical to the ECL signal intensity of CdTe@CdS QDs. Thiourea, as a classic •OH scavenger, was used to confirm the production of •OH during the ECL processes (Chen et al., 2016, 2017a, 2017b). As shown in Fig. 3A, the thiourea addition results a significant decrease of ECL intensity, verifying the generation of hydroxyl radicals. Then, catalase was used to identify the crucial role of H_2O_2 because catalase can catalyze H_2O_2 decomposition into oxygen and water which effectively eliminates H_2O_2 around electrode interface (Ghiretti, 1956). As shown in Fig. 3B, the ECL signal decreases significantly after catalase was added, indicating that H_2O_2 would directly oxidize CdTe@CdS QDs and result in excited state CdTe@CdS* formation. Those experimental results demonstrate that •OH and H_2O_2 are involved with the whole ECL processes of CdTe@CdS QDs.

As the proposed CoA-Ag complexes display outstanding amplification to the ECL of CdTe@CdS QDs, the definite role of CoA-Ag complex among the enhancing process deserves insight investigations. Once thiourea (Fig. 3C) or catalase (Fig. 3D) was added into CoA-Ag complex system, both of the ECL signal decrease clearly indicating that hydroxyl radicals and H_2O_2 are still involved in ECL processes. Namely, the modification of CoA-Ag complex does not alter the fundamental ECL generation process of CdTe@CdS QDs. According to the ECL mechanism mentioned in Eqs. (1)–(5), the signal intensity depends on the yielding rate of the excited state (CdTe@CdS*) that mainly derived from the combination of •OH and charged radicals (CdTe@CdS(e^-)). While, CoA-Ag complex modification results in an evidently CV current increase as shown in Fig. 2B, suggesting electron transfer rate among ECL processes being accelerated. Therefore, accelerated electron transferring induced CdTe@CdS(e^-) and •OH producing rates increasing are reasoned to be the main factors for ECL amplification.

In addition to electron transferring factor, effects of various possible groups in CoA-Ag complex such as mercapto, phosphate and adenine bases on the ECL signal of CdTe@CdS QDs also draw our attention. As shown in Fig. 4A, mercapto-containing substances (BSA, Cys, GSH and DTT) and adenine derivatives with different phosphoryl groups (adenosine triphosphate (ATP), adenosine diphosphate (ADP) and adenosine monophosphate (AMP)) exhibit almost little amplification or even quenching effects on the ECL signal, indicating that the ECL enhancement actually results from substantial reaction of CoA-Ag complex. According to the reported literature (Bockris and Oldfield, 1955; Vaik et al., 2004), H_2O_2 electrochemical reduction will produce abundant reactive hydroxyl radicals essential for ECL emission according to Eq. (6) and (7). Combining the electrical catalytic role of noble metal material such as Pt, Au and Ag particles (Valenti et al., 2018; Zhou et al., 2017) with the electron transfer rate increase facts during ECL scanning, we hypothesize that the excellent electrocatalytic reduction H_2O_2 activity derived from CoA-Ag complex would play a major role in ECL

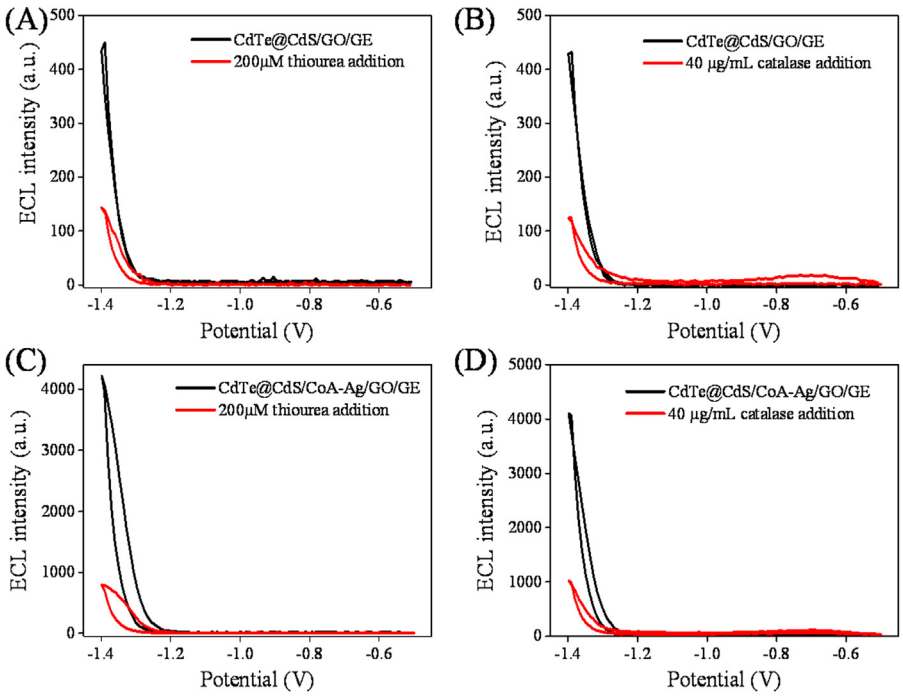

Fig. 3. (A) ECL responses of CdTe@CdS/GO/GE before (black line) and after (red line) the addition of 200 μM thiourea. (B) ECL responses of CdTe@CdS/GO/GE before (black line) and after (red line) the addition of 40 μg mL^{-1} catalase. (C) ECL responses of CdTe@CdS/CoA-Ag/GO/GE before (black line) and after (red line) the addition of 200 μM thiourea. (D) ECL responses of CdTe@CdS/CoA-Ag/GO/GE before (black line) and after (red line) the addition of 40 μg mL^{-1} catalase (For interpretation of the references to color in this figure legend, the reader is referred to the web version of this article).

signal amplification. As shown in Fig. 4B, CoA-Ag/GO/GE exhibits a strong and enhanced H_2O_2 reduction CV peak current (about −1.1 V vs Ag/AgCl) in comparison with that of single GO/GE and bare electrode, which confirmed good electrocatalytic reduction H_2O_2 activity of CoA-Ag complex. Therefore, we concluded that the enhanced electron transfer abilities and perfect electrochemical catalysis of CoA-Ag complex lead to the final ECL amplification toward CdTe@CdS QDs.

3.4. CoA quantitative analysis

The amounts of CoA-Ag complex determine the electrochemical catalytic ECL enhancement towards CdTe@CdS QDs. Some experimental parameters have been optimized. As shown in Fig. S7, acceptable operation dosage of CdTe@CdS QDs and CoA-Ag complex are found to 2 μL each other. Considering the concentration of CoA-Ag

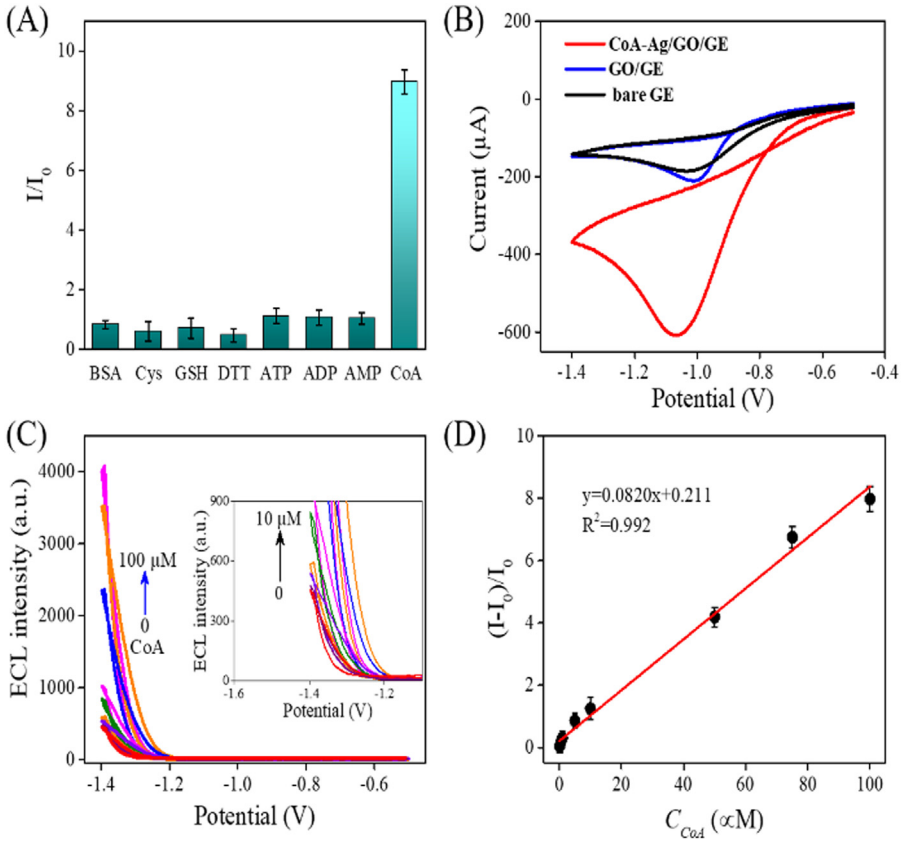

Fig. 4. (A) The ECL signals of the proposed sensor in response to CoA, other thiol-containing ligands (BSA, cysteine (Cys), glutathione (GSH) and dithiothreitol (DTT)), and other adenine-containing ligands (adenine, adenosine triphosphate (ATP), adenosine diphosphate (ADP) and adenosine monophosphate (AMP)), the concentration of all ligands was equal to Ag^+ which was 100 μM. (B) Cyclic voltammogram of H_2O_2 reduction proceeded on bare glassy electrode (GE, black line), GO deposited glassy electrode (GO/GE, blue line) and CoA-Ag complex modified GO/GE (CoA-Ag/GO/GE, red line). (C) ECL-potential curves of CdTe@CdS/CoA-Ag/GO/GE in the presence of H_2O_2 (5 mM) PBS (pH 8.0) with different CoA concentrations (from bottom to top: 0, 0.1, 0.5, 1, 5, 10, 50, 75 and 100 μM, inset shows the enlarge curves from 0 to 10 μM) and the fixed $AgNO_3$ concentration (100 μM). (D) Plot of ECL-potential peak intensity versus CoA concentrations (For interpretation of the references to color in this figure legend, the reader is referred to the web version of this article).

complex was controlled by the concentrations of Ag^+ and CoA, a kind of signal-on strategy for CoA analysis is sought to investigate the relationships between CoA and ECL signals of CdTe@CdS QDs. As shown in Fig. 4C, the ECL signal increases with the increase of CoA concentration within a range of 0.1 ~ 100 μM, which is due to the increase of CoA-Ag complex amount. Depending on the ECL intensities under different concentrations of CoA, a linear relationship between ECL signals and CoA concentration is plotted in Fig. 4D. The linear equation is calculated: $I\text{-}I_0/I_0 = 0.0820\,C + 0.211$ (where I_0 presents the initial ECL intensity, I presents CoA-Ag modified ECL intensity) with the limit of detection (LOD) of 0.03 μM (S/N = 3). The proposed ECL method was compared with other reported methods. As depicted in Table S1, the detectable concentration range was wider than that of colorimetric method (Wu et al., 2016) and the LOD was comparable to that of fluorescent strategy (Hu et al., 2017a), photoelectronchemical method (Zhao et al., 2018) and traditional electrochemical method (Hu et al., 2015; Wang et al., 2016). To further explore the feasible application on sensing in the biological sample, we added 10% serum into the reaction system while fixing other reactants. The contents of each sample calculated from the calibration curve were compared with those obtained using the CoA assay kit, and satisfactory data in Table S2. The results in Table S2 show that the recovery of CoA is between 98% and 107% and detection value is comparable to that of the assay kit, indicating the constructed signal-on sensor has favorable potential for realistic sample detection.

3.5. Acetyltransferase activity sensing

Based on the unique ECL amplification properties of the CoA-Ag complex, a kind of ECL sensor was fabricated to detect the activity of acetyltransferase (Scheme 1). HAT p300 was selected as the reaction model. HAT p300 transfers the acetyl group from acetyl-CoA (Ac-CoA) to the lysine of substrate polypeptides (H4), and to produce CoA (Biel et al., 2005; Han et al., 2015). The generated CoA coordinates with Ag^+ to form CoA-Ag complex afterwards. Prior to sensing construction, the ECL feasibility for acetyltransferase activity analysis was investigated (Fig. S8). In the presence of p300, Ag^+, Ac-CoA or substrate polypeptides H4 alone, the ECL signal weakly changes in comparison with CdTe@CdS QDs, suggesting little interference caused by the reaction substrates. Only under the coexistence of p300, Ag^+, Ac-CoA and H4 polypeptides (Fig. 5A), the ECL intensity is significantly amplified. Acetyltransferase p300 (0–150 nM) catalyze the reaction between Ac-CoA and H4 peptide to produce CoA that reacts with Ag^+ to form CoA-Ag complex to accelerate electron transferring and catalyze H_2O_2 reduction, which finally results in an enhanced ECL signal of CdTe@CdS QDs. According to the relationship between different p300 concentrations and the corresponding ECL signal intensities, a good linear relationship is generated among the concentration range from 0.1 to 100 nM with a LOD of 0.05 nM, which is comparable to the traditional electrochemical methods (Hu et al., 2015). After all, a sensitive signal-on ECL biosensor based on CoA-Ag complex sensitized ECL of CdTe@CdS QDs was designed and exhibited promising capability for acetyltransferase determination.

3.6. Inhibitor screening

It is of great importance to screen and assess the inhibitors of HAT in the therapeutic application, as dysfunction of histone acetylation and the aberrant activity of HATs/HDACs is often associated with the pathogenesis of numerous diseases, especially cancer (Liu et al., 2002; Ozturk et al., 2006). Therefore, a potential HAT p300 inhibitor, anacardic acid was applied to evaluate the feasibility of the proposed ECL

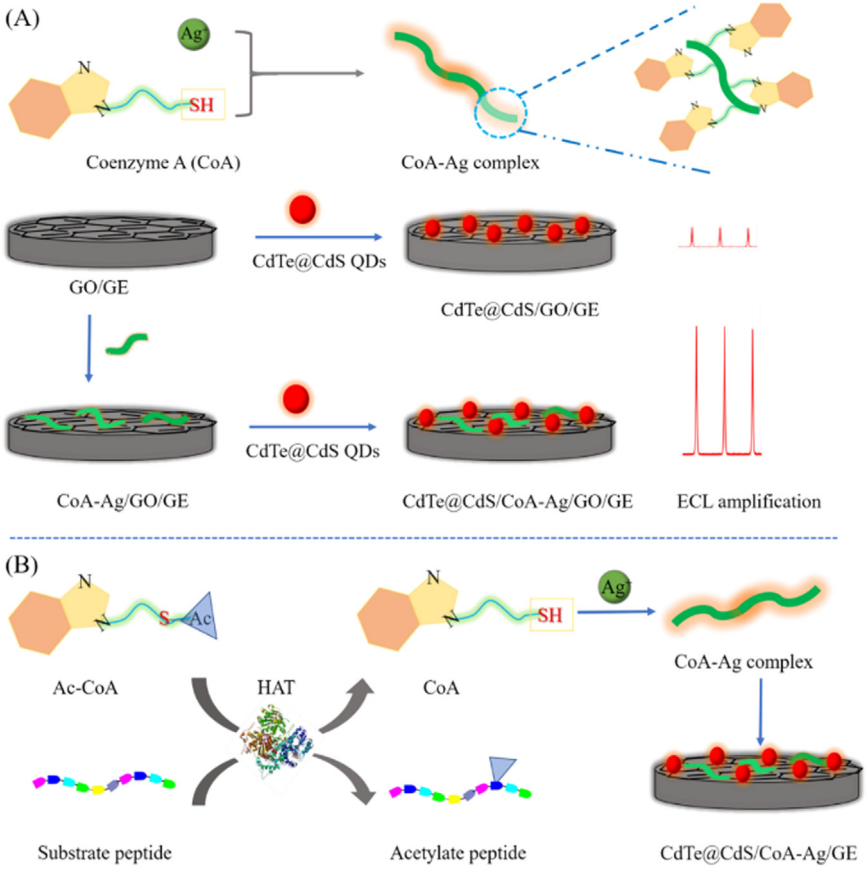

Scheme 1. Schematic diagrams of (A) the synthesis of CoA-Ag(I) CP and its ECL detection on GO modified electrode and (B) the ECL biosensor for probing HAT activity.

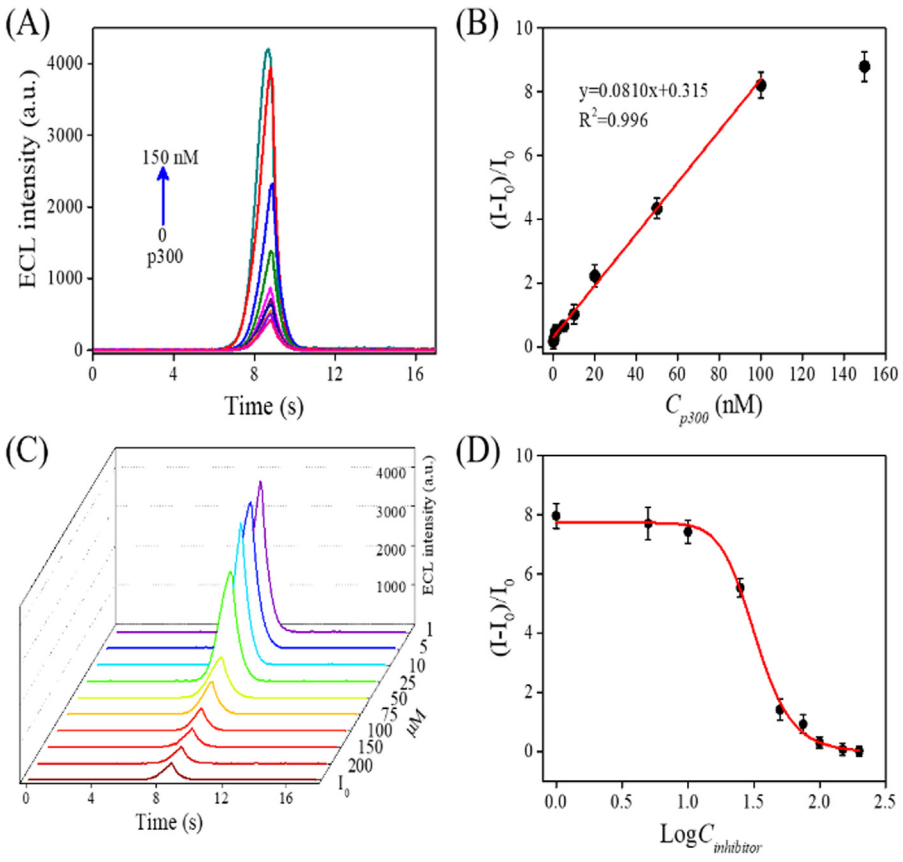

Fig. 5. ECL detection of HAT at the CdTe@CdS/CoA-Ag/GO/GE in 200 mM PBS (pH 8.0) with 5 mM H_2O_2: (A) ECL intensity-time response to different concentrations of p300 HAT (From top to bottom: 0, 0.1, 0.5, 1.0, 5.0, 10, 20, 50, 100 and 150 nM); (B) Calibration curve of the proposed HAT sensor. ECL detection of HAT inhibition at the CdTe@CdS/CoA-Ag/GO/GE in 200 mM PBS (pH 8.0) with 5 mM H_2O_2: (C) ECL intensity-time response to different concentrations of anacardic acid; (D) ECL signal as a function of the concentration of anacradic acid (1.0, 5.0, 10, 25, 50, 75, 100, 150, and 200 μM).

sensor on inhibitors assessing. As shown in Fig. 5C, p300 activity is clearly inhibited along with the addition of anacardic acid, and the relevant ECL signal decreases compliance with increasement of anacardic acid. Meanwhile, the relationship between the ECL responses and the anacardic acid concentrations is plotted in Fig. 5D. The IC_{50} value (half maximal inhibitory concentration) is calculated to be 32.6 ± 2.0 μM, which is consistent with that in other literatures (Chen et al., 2015b; Hu et al., 2015). These observations clearly suggest that the proposed CoA-Ag complex based ECL sensor can be used to quantitatively assess HAT inhibitors.

3.7. Selectivity of the proposed sensor

Favorable selectivity is crucial for a biosensor. Consequently, the selectivity of this HAT biosensor was evaluated with other common control enzymes or interfering factors proteins: carboxypeptidase (CPY), thrombin (Thrombin), protein kinase (PKA), lysozyme and Sortase A. Fig. S9 shows that the ECL signal for HAT p300 is much higher than that of other enzymes which cannot catalyze the occurrence of acetylation and produce CoA to form CoA-Ag complex, implying an excellent selectivity of the proposed HAT biosensor. The above results also demonstrate that the CoA-Ag complex induced signal-on ECL sensor is a potent platform for sensitive detection of HAT p300.

4. Conclusions

In summary, CoA-Ag complex was developed in situ and verified to accelerate the electron transferring and electrochemical catalysis H_2O_2 decomposition to enhance the cathode ECL intensity of CdTe@CdS QDs. Afterward, a convenient label-free signal-on ECL approach for CoA detection was constructed with exhibit excellent specificity to CoA. In addition, this method further exhibits the feasibility to detect HAT activity and screen relevant inhibitors, exhibiting a promising potential in the practical application of HAT based biochemical research, disease diagnosis and drug discovery.

Acknowledgment

This work was financially supported by the National Natural Science Foundation of China (Nos. 21305037, 21475037, and 21804145).

Appendix A. Supporting information

Supplementary data associated with this article can be found in the online version at doi:10.1016/j.bios.2018.11.003.

References

Bae, Y., Myung, N., Bard, A.J., 2004. Nano Lett. 4 (6), 1153–1161.
Benoit, L., Choi, J.P., 2017. ChemElectroChem 4 (7), 1573–1586.
Biel, M., Wascholowski, V., Giannis, A., 2005. Angew. Chem. Int. Ed. 117 (21), 3248–3280.
Bockris, J.O.M., Oldfield, L.F., 1955. Trans. Faraday Soc. 51 (0), 249–259.
Chen, H., Li, W., Wang, Q., Jin, X., Nie, Z., Yao, S., 2016. Electrochim. Acta 214 (1), 94–102.
Chen, H., Li, W., Zhao, P., Nie, Z., Yao, S., 2015a. Electrochim. Acta 178 (1), 407–413.
Chen, H., Wang, Q., Shen, Q., Liu, X., Li, W., Nie, Z., Yao, S., 2017a. Biosens. Bioelectron. 91, 878–884.
Chen, Y., Wang, X., Cao, X., Zhao, Y., 2017b. Anal. Chem. 89 (19), 10468–10473.
Chen, L., Wang, J., Li, W., Han, H., 2012. Chem. Commun. 48 (41), 4971–4973.
Chen, S., Li, Y., Hu, Y., Han, Y., Huang, Y., Nie, Z., Yao, S., 2015b. Chem. Commun. 51 (21), 4469–4472.
Ding, C., Zhang, W., Wang, W., Chen, Y., Li, X., 2015. TrAC, Trends Anal. Chem. 65, 137–150.
Gao, T., Yang, C., Zheng, Y., 2013. Anal. Bioanal. Chem. 405 (4), 1361–1371.
Ghadiali, J.E., Lowe, S.B., Stevens, M.M., 2011. Angew. Chem. Int. Ed. 123 (15), 3479–3482.
Ghiretti, F., 1956. Arch. Biochem. Biophys. 63 (1), 165–176.
Han, Y., Li, P., Xu, Y., Li, H., Song, Z., Nie, Z., Chen, Z., Yao, S., 2015. Small 11 (7), 877–885.
He, L., Wu, M., Xu, J., Chen, H., 2013. Chem. Commun. 49 (15), 1539–1541.
Hu, Y., Chen, S., Han, Y., Chen, H., Wang, Q., Nie, Z., Huang, Y., Yao, S., 2015. Chem.

Commun. 51 (99), 17611–17614.
Hu, Y., Zhang, L., Li, X., Liu, R., Lin, L., Zhao, S., 2017a. ACS Sustain. Chem. Eng. 5, 4992–5000.
Hu, Y., Zhang, Q., Guo, Z., Wang, S., 2017b. J. Electroanal. Chem. 801, 306–314.
Hummers, W.S., Offeman, R.E., 1958. J. Am. Chem. Soc. 80 (6) (1339-1339).
Jie, G., Liu, B., Miao, J., Zhu, J., 2007. Talanta 71 (4), 1476–1480.
Jie, G., Tan, L., Zhao, Y., Wang, X., 2017. Biosens. Bioelectron. 94, 243–249.
Kuninger, D., Lundblad, J., Semirale, A., Rotwein, P., 2007. J. Biotechnol. 131 (3), 253–260.
Li, P., Han, Y., Li, Y., Zhu, R., Wang, H., Nie, Z., Yao, S., 2016. Anal. Bioanal. Chem. 16, 9304–9310.
Liu, J., Killilea, D.W., Ames, B.N., 2002. PNAS 99 (4), 1876.
Liu, Z., Qi, W., Xu, G., 2015. Chem. Soc. Rev. 44 (10), 3117–3142.
Ma, S., Hu, Y., Zhang, Q., Guo, Z., Wang, S., Shen, Q., Liu, C., Liu, Z., 2018. Sens. Actuators, B 273, 760–770.
MacDonald, M.A., Zhang, P., Chen, N., Qian, H., Jin, R., 2011. J. Phys. Chem. C. 115 (1), 65–69.
Mishra, P.K., Drueckhammer, D.G., 2000. Chem. Rev. 100 (9), 3283–3310.
Ozturk, A., DeKosky, S.T., Kamboh, M.I., 2006. Neurobiol. Aging 27 (10), 1440–1444.
Pei, H., Lu, N., Wen, Y., Song, S., Liu, Y., Yan, H., Fan, C., 2010. Adv. Mater. 22, 4754–4758.
Pei, H., Wan, Y., Li, J., Hu, H., Su, Y., Huang, Q., Fan, C., 2011. Chem. Commun. 47, 6254–6256.
Trievel, R.C., Li, F., Marmorstein, R., 2000. Anal. Biochem. 287 (2), 319–328.
Vaik, K., Schiffrin, D.J., Tammeveski, K., 2004. Electrochem. Commun. 6 (1), 1–5.
Valenti, G., Rampazzo, E., Kesarkar, S., Genovese, D., Fiorani, A., Zanut, A., Palomba, F., Marcaccio, M., Paolucci, F., Prodi, L., 2018. Coord. Chem. Rev. 367, 65–81.
Wang, Q., Chen, H., Li, Y., Wang, H., Nie, Z., Hu, Y., Yao, S., 2016. Talanta 161, 583–591.
Wang, Y., Chen, Y., Wang, H., Cheng, Y., Zhao, X., 2015. Anal. Chem. 87 (10), 5046–5049.
Wang, X., Chen, F., Zhang, D., Zhao, Y., Wei, J., Wang, L., Song, S., Fan, C., Zhao, Y., 2017. Chem. Sci. 8, 4764–4770.
Wu, R., Liao, L., Li, S., Yang, Y., Xiao, X., Nie, C., 2016. Microchim. Acta 183, 715–721.
Wu, H., Liu, S., Zhu, W., Jiang, J., Shen, G., Yu, R., 2012. Electroanalysis 24 (12), 2365–2370.
Wu, J., Zheng, Y., 2008. Anal. Biochem. 380 (1), 106–110.
Xu, L., Zhang, W., Shang, L., Ma, R., Jia, L., Jia, W., Wang, H., Niu, L., 2018. Biosens. Bioelectron. 103, 6–11.
Yuan, X., Tay, Y., Dou, X., Luo, Z., Leong, D.T., Xie, J., 2013. Anal. Chem. 85 (3), 1913–1919.
Zhao, C., Kong, Y., Liu, L., Wang, X., 2018. Electrochim. Acta 273, 10–16.
Zhen, Z., Tang, L., Long, H., Jiang, J., 2012. Anal. Chem. 84 (8), 3614–3620.
Zheng, Y., Dou, X., Li, H., Lin, J., 2016. Nanoscale 8 (9), 4933–4937.
Zhou, Y., Wang, H., Zhuo, Y., Chai, Y., Yuan, R., 2017. Anal. Chem. 89 (6), 3732–3738.